

Fabrication and Characterization of Interconnected Nanowell Molecular Electronic Devices in Crossbar Architecture

Zena L. Martin, Nabanita Majumdar, Michael J. Cabral, Nadine Gergel-Hackett, Fernanda Camacho-Alanis, Nathan Swami, John C. Bean, *Fellow, IEEE*, Lloyd R. Harriott, Y. Yao, James M. Tour, D. Long, and R. Shashidhar

Abstract—The implementation of circuit architectures based on molecular electronic devices has been impeded by the availability of facile fabrication schemes for the interconnection of individual devices. The deposition and patterning of a top contact layer between adjoining devices for interconnection purposes can result in contacts of poor fidelity, which introduces artifacts in the I - V characteristics that are not attributable to molecular transport between the contacts. In this study, through the fabrication of interconnected devices within the crossbar device architecture, we demonstrate that the vapor-phase molecular deposition method for fabrication of device layers was compatible with the massively parallel microelectronic fabrication process of liftoff, for patterning of contact layers. A prepatterned device with Au bottom contacts, as well as a bilayer resist for patterning the top Au contacts through postdeposition liftoff was used as the substrate for vapor-phase deposition of a monolayer of conjugated oligo-(phenylene ethynylene) (plain-OPE) molecules and patterning of the top metal contact layer. Interconnection in series and parallel configurations was confirmed by I - V characteristics similar to classical resistors with equivalent conductivity of each individual molecular device. Additionally, to better understand molecular transport in the device junctions, we performed temperature-dependent I - V studies on individual molecular devices that were fabricated using prepatterned Au bottom contacts as the substrate for solution-phase deposition of the molecular monolayer, onto which the Au top contacts were evaporated and patterned using a shadow mask. Molecular layers of two distinctly different room-temperature I - V characteristics, including nonswitching plain-OPE and switching nitro-OPE molecular devices, were used to study the fidelity of the molecular junctions. Based on the persistence of the device characteristics of both types of molecular layers down to 100 K, and in particular, the observation of switching between “high” and “low” conductivity states at characteristic threshold voltages at all temperatures, only

with nitro-OPE molecular devices, and not with plain-OPE molecular devices, we conclude that the observed transport was a characteristic molecular signature not dependent on filament formation at contacts.

Index Terms—Electrical contacts, interconnected devices, molecular electronics, semiconductor device fabrication.

I. INTRODUCTION

DEVICES and circuits based on molecular electronics are now on the International Technology Roadmap for Semiconductors (ITRS) [1], [2] for scaling below ~ 30 nm, where performance gains are expected to be severely limited. In spite of several proposals for circuit architectures based on molecular electronics [3]–[6], barring those based on charge storage memory devices [7], [8], few others have been implemented. A major challenge in fabricating the circuit is the fidelity of the contacts [9] upon interconnection of molecular devices, since the deposition and patterning of a top contact layer between adjoining devices impedes the chemical stability and electronic coupling at metal–molecule junctions [10]–[12], resulting in artifacts in the I - V characteristics due to filament formation rather than the molecular nature of phenomena at the contacts. Prior work has demonstrated the fabrication of interconnected molecular devices in a crossbar architecture using methods such as imprint lithography [13]–[15] or nanowire assembly techniques [16], which can be made compatible with molecules in the device structure. However, multiple process steps and masks are required for contact patterning; the devices are not well suited to vertical integration due to exposed edges, and there is much debate on the role of filaments in the I - V characteristics of these structures [17]. Contact and interconnect patterning process strategies based on the commonly used microelectronic fabrication techniques of liftoff or etching require that the electron-beam or photolithographically patterned resists be compatible with the deposition step for molecular self-assembled monolayers (SAMs). However, most prepatterned resists dissolve in the liquid-phase SAM deposition solution. The microelectronics industry has traditionally benefited from gas-phase processing methods for deposition and etching, since these offer far superior uniformity and reproducibility than liquid-phase methods. This motivates us to consider the application of vapor phase molecular monolayer deposition in conjunction with liftoff techniques for contact patterning, using a sealed nanowell device structure [18], to ensure insulation

Manuscript received September 1, 2008; revised March 4, 2009. First published May 2, 2009; current version published September 4, 2009. This work was supported in part by the National Science Foundation under Award ECCS 0701505 and in part by the Defense Advanced Research Projects Agency/Office of Naval Research (DARPA/ONR) MoleApps program (N00014010706). The review of this paper was arranged by Associate Editor M. P. Anantram.

Z. L. Martin and N. Majumdar were with the University of Virginia (UVA), Charlottesville, VA 22904 USA.

M. J. Cabral, F. Camacho-Alanis, N. Swami, J. C. Bean, and L. R. Harriott are with the University of Virginia (UVA), Charlottesville, VA 22904 USA (e-mail: nswami@virginia.edu).

N. Gergel-Hackett was with the University of Virginia (UVA), Charlottesville, VA 22904 USA. She is now with the National Institute of Standards and Technology, Gaithersburg, MD 20899 USA.

Y. Yao was with the Rice University, Houston, TX 77005 USA. He is now with Sigma-Aldrich, Madison, WI 53711 USA.

J. M. Tour is with the Rice University, Houston, TX 77005 USA.

D. Long and R. Shashidhar were with the Geo Centers, Arlington, VA 22209 USA.

Color versions of one or more of the figures in this paper are available online at <http://ieeexplore.ieee.org>.

Digital Object Identifier 10.1109/TNANO.2009.2021161

of device layers from the atmosphere and each other, thereby enabling compatibility to subsequent vertical integration. Such process strategies for interconnection are likely necessary for the construction of molecular circuits to a level of complexity that is eventually necessary for computational memory [19] and logic circuits paradigms [20].

In this study, we report on the fabrication of one type of interconnected molecular device using vapor-phase deposition of a molecular monolayer onto a planar nanowell device structure with Au bottom contacts, followed by application of the massively parallel microelectronic liftoff technique to pattern the Au top contacts. Central to the fabrication strategy was the use of a prefabricated device substrate that was prepatterned with bottom contacts as well as a bilayer resist for top contact patterning through postdeposition liftoff. Vapor-phase deposition methods were used to form a uniform monolayer of conjugated molecules of oligo-(phenylene ethynylene) (plain-OPE) on the prefabricated substrate, followed by top metal deposition and resist liftoff to pattern the top metal. In this manner, we demonstrate that vapor-phase molecular deposition methods for device layers were compatible with the resists used for patterning of contact layers by liftoff and etch techniques, and the molecules of the SAM were subject to minimal damage due to the deposition and patterning step for the top contact. Interconnection of molecular devices in series and parallel configurations was confirmed by I - V characteristics that were similar to classical resistors with equivalent conductivity of each individual molecular device, thereby attesting to the fidelity of contacts since I - V characteristics of the individual devices were preserved upon interconnection.

Temperature-dependent I - V studies can aid in the distinction of molecular transport from transport due to filament artifacts, since the latter usually does not persist down to low temperatures [21]. Hence, to better understand molecular transport of the nanowell device structure, a second set of individual (rather than interconnected) molecular devices was fabricated using prepatterned bottom gold contacts as the substrate for solution-phase deposition of molecular monolayers with two distinctly different room-temperature I - V characteristics, followed by evaporation and patterning of top contacts on the respective molecular layer using a shadow mask. Prior work on room-temperature I - V characteristics of these molecular devices has shown that devices with plain-OPE SAMs did not exhibit variations in conductivity based on the history of the voltage sweep; whereas devices with nitro-OPE SAMs showed switching between the “high” and “low” conductivity states at characteristic threshold voltages [22]–[24]. Through temperature-dependent I - V studies we aimed to test if these room-temperature device characteristics persist down to lower temperatures, where transport due to processes such as filament formation was less likely. The resulting I - V characteristics confirm that switching from “high” to “low” conductivity states at characteristic temperature-dependent threshold voltages was observed at all temperatures down to 100 K, *only* with nitro-OPE molecular devices; and switching was *never* observed at low or room temperatures with plain-OPE molecular devices. Based on the persistence of the device characteristics of both plain-OPE and

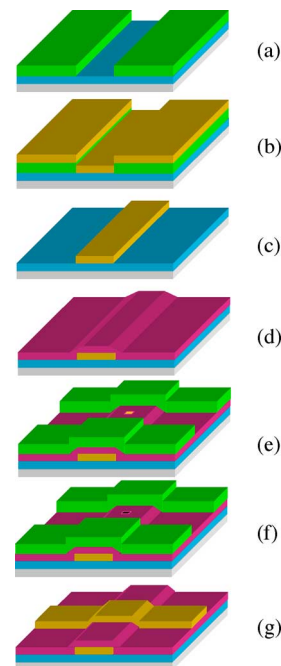


Fig. 1. Schematic process flow for fabrication of crossbar nanowell molecular devices. (a) Photoresist patterning for bottom contacts on SiO_2 (50 nm) / Si wafer. (b) Deposition of 5 nm of Ti and 200 nm Au over patterned substrate. (c) Lifting off excess Au with removal photoresist. (d) Deposition of 100 nm of HPD-CVD Si_3N_4 over the entire substrate. (e) Photoresist patterning for top contact, followed by FIB milling ($100 \text{ nm} \times 10 \text{ nm}$). (f) Vapor deposition of molecules into the FIB-milled holes. (g) Deposition of 5 nm of Ti and 200 nm Au over the entire substrate and lifting off excess Au with removal of photoresist to serve as top-contacts.

nitro-OPE devices down to low temperatures, we conclude that the transport mechanism observed within our device structure was a characteristic molecular signature of the particular type of molecular layer within the device structure and not of processes at the contacts, such as filaments.

II. EXPERIMENTAL METHODS

A. Fabrication of Interconnected Nanowell Crossbar Molecular Devices

Vapor-phase methods for the deposition of plain-OPE monolayers have been described previously [26]. We present here a summary of how this process was integrated with the microelectronic liftoff technique to form a patterned top contact on the molecular monolayer to enable the construction of a crossbar architecture, as shown in Fig. 1.

Step 1: Lithography for bottom electrodes was accomplished by starting with a clean single-side polished silicon substrate onto which a thin layer of hexamethyldisilazane (HMDS) was vapor deposited to promote photoresist adhesion to the oxide surface. Photoresist AZ 5214 was spun on at 6000 r/min for 30 s, and left to dry and then baked at 100°C for 2 min. The resist was exposed using the appropriate mask pattern in a Karl Suss, DUV mask aligner (320 nm wavelength) for 18 s, and developed in diluted AZ 400 K (1:4) for 30–40 s to form the pattern for the bottom electrode lines.

- Step 2:** Metal deposition and liftoff: 5 nm of titanium and 200 nm of gold were deposited by electron-beam evaporation on the photoresist-patterned wafer and the wafer was submerged in acetone to remove the photoresist and the excess metal adhered on the resist.
- Step 3:** Silicon nitride deposition was accomplished using high-density plasma-enhanced chemical vapor deposition (PECVD) to form a uniform pinhole-free 100 nm layer.
- Step 4:** Photolithography to expose bond pad areas for electrical probing was done by standard wet or dry-etch methods for silicon nitride to expose 200 μm square pads.
- Step 5:** Prepatterning resist for top contact was accomplished similar to Step 1, except that the use of a bilayer resist process was vital to the fabrication of the resist overhang profile that is necessary for easy lift off of metal after SAM deposition, as is described in greater detail in Section III. First, HDMS was used to promote adhesion of the resist AZ 4110, which was spun on at 5000 r/min for 30 s and baked at 100 $^{\circ}\text{C}$ for 1 min. The resist was flood-exposed in the Karl Suss, DUV aligner for 18 s. A second resist, AZ 4210, was spun on at 5000 r/min for 30 s, baked at 100 $^{\circ}\text{C}$ for 1 min, and exposed to the appropriate pattern in the Karl Suss DUV aligner for 90 s. The resists were then developed in diluted AZ 400 K (1:4) for 30–40 s and rinsed in deionized (DI) water to form the patterned area for postdeposition liftoff.
- Step 6:** Active regions for deposition of the molecular layer were milled using a gallium-focused ion beam (FEI FIB 200) with an 8-nm diameter to mill 30- to 100-nm-sized square wells through the 100-nm-thick silicon nitride film. Direct-write electron beam lithography could also be used for this step.
- Step 7:** Vapor-phase deposition of plain-OPE molecular layers was accomplished as described previously [26], in an ultrahigh vacuum (UHV) chamber (5×10^{-9} Torr), with a cold cathode gauge for measurement of the pressure, and a low-temperature thermal cell that was optimized for performance in the ~ 100 to 130 $^{\circ}\text{C}$ temperature range, with less than 0.4 $^{\circ}\text{C}$ of overshoot for improved temperature control. For deposition of the molecular layer, the temperature of the thermal cell was ramped up to 80 $^{\circ}\text{C}$, and the gold surface of the substrate in the deposition chamber was placed to face the source and at a separation of 8 cm. The flux of impinging molecules was varied by changing either the exposure time or the source temperature, and these were optimized to determine the conditions required for deposition of a chemisorbed monolayer, by various surface analysis methodologies. The Au top-contact was deposited in an e-beam evaporator (pressure $\sim 1 \times 10^{-6}$ Torr) where the source was ~ 35 cm away from the substrate. To ensure complete wetting of the nanowell by vapor-deposited metal, a thin adhesion layer of titanium (< 5 nm) deposited at 1 $\text{\AA}/\text{s}$ was necessary, prior to deposition of 200 nm Au at 10 $\text{\AA}/\text{s}$ on the monolayer.
- Step 8:** Top metal liftoff in acetone was similar to Step 2.

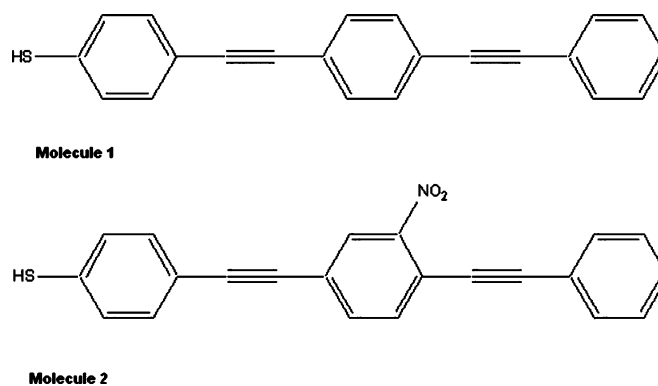


Fig. 2. Molecules used within the device structure: plain-OPE (molecule 1) and nitro-OPE (molecule 2).

B. Fabrication of Individual Nanowell Crossbar Molecular Devices

To distinguish between transport due to molecular phenomena and transport involving metal filaments, temperature-dependent I – V characteristics of devices composed of molecular layers with distinctly different room-temperature characteristics were studied at low temperatures (100 K). Unlike devices with metal filaments, devices with molecular-dependent I – V characteristics would be expected to retain their distinct electrical behavior, even as the ambient temperature decreases. For this purpose, devices composed of nonswitching plain-OPE molecules were compared to those of the switching nitro-OPE molecules (molecular structures shown in Fig. 2). Since vapor-phase deposition of nitro-OPE SAMs was not possible, we used liquid-phase process for deposition of these SAMs. However, since the liquid-phase SAM deposition method was not compatible with the “liftoff” resists used to enable interconnection, the temperature-dependent I – V studies were conducted by comparing individual nanowell (rather than interconnected) molecular devices composed of liquid-phase deposited nitro-OPE and plain-OPE molecular layers. We also confirmed that the I – V characteristics of plain-OPE devices fabricated by vapor-phase deposition matched those obtained with liquid-phase deposition. To ensure a large number of working molecular device junctions (no “short” or “open” devices) on Au surfaces, the devices need to be constructed on a portion of the Au surface with no defects and which is less likely to form filaments. Hence, the nanowell device structure is required so that the SAMs do not extend over a grain boundary of the Au surface where such defects are likely, whereas the same is not required for molecular device junctions constructed on single-crystal semiconductor surfaces, where a high device yield may be obtained even with micron-sized wells [25]. Fabrication of the individual nanowell molecular devices by liquid-phase deposition methods has been described previously [24], as well as the room-temperature I – V characterization of switching properties of the nitro-OPE versus plain-OPE monolayers [27]. Briefly, a gallium-FIB (FEI FIB 200) with an 8-nm diameter was used to mill 30- to 100-nm-sized square wells through the 100-nm-thick silicon nitride film to form a nanowell of prepatterned bottom gold substrates for

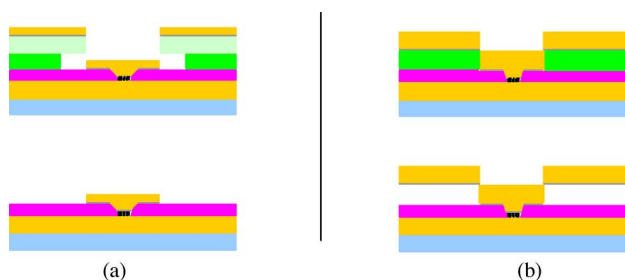


Fig. 3. Cross-section drawing of liftoff process. (a) Photoresist overhang using bilayer process makes clean pattern on substrate. (b) Lack of photoresist overhang can lead to excess metal staying on the substrate.

solution-phase deposition of molecular monolayers. This was followed by evaporation and patterning of top contacts on the respective molecular layer using a shadow mask.

C. Characterization of Individual and Interconnected Nanowell Crossbar Devices

Temperature-dependent I - V characteristics of the molecular devices were acquired using a standard semiconductor parameter analyzer (HP 4145 B) on a cryostat modulated between 20 K and room temperature, to probe the respective pads for the top and bottom contacts to the molecule. Following the identification of pads with molecular device response in their I - V characteristics (confirmed through Simmons equation analysis), experiments on interconnected molecular devices in series and parallel were conducted as described in the following section.

III. RESULTS AND DISCUSSION

A. Fabrication of Resist Overhang for Lift Off

The liftoff step in acetone to remove the resist and metal adhered to it, without destroying the metal contact layer or the vapor-phase-deposited SAM layer, was a crucial step in the device fabrication process. Vital to this step was a resist overhang that permitted the lift off to occur easily, without the need for agitation or high temperatures, since these were destructive to the SAMs. Fig. 3(a) schematically shows how the overhang facilitates a patterned metal overlayer to remain *only* in the region neighboring the SAMs, while Fig. 3(b) schematically shows how the lack of an overhang can lead to an excess metal overlayer remaining on portions of the substrate other than the area neighboring the SAM, thereby causing electrical shorts. Fig. 4(a) schematically shows the expected resist pattern on all areas except within the central lines where Au lines are needed for the top contact, and Fig. 4(b) shows the secondary electron emission image from the FIB, showing the bilayer resist edge in those areas.

B. Vapor-Phase Deposition of OPE SAMs

Another unique attribute of this study was the use of vapor-phase techniques to deposit a uniform layer of plain-OPE SAMs. This was necessary since liquid-phase deposition methods interfere with the prepatterned resist, thereby destroying the patterns or contaminating the active area designed for SAM deposition,

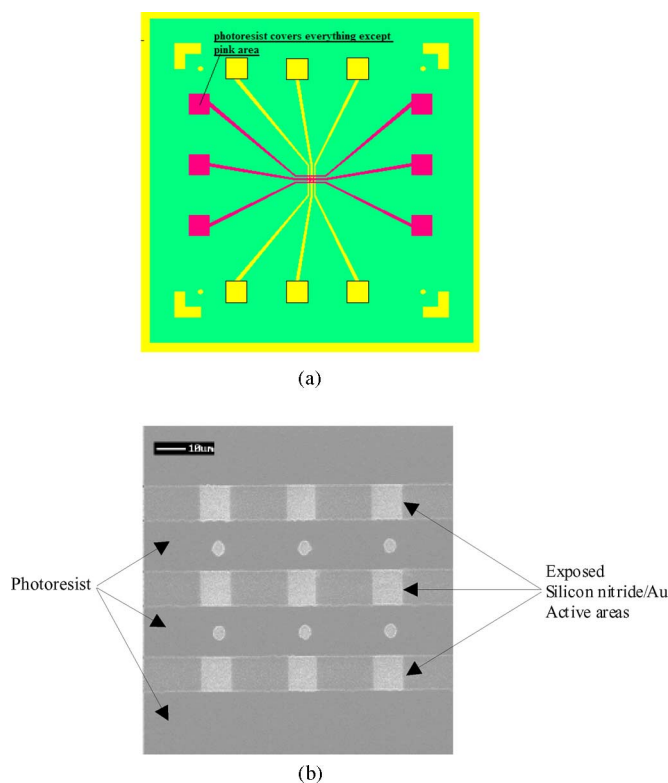


Fig. 4. (a) Schematic of bilayer photoresist covering all areas except the dark shaded region (in red for color version). The underlying patterned gold (light shade) and silicon nitride (grey shade) layers are also shown for comparison. (b) Secondary electron emission image (10 μm scale marker) from the FIB showing the bilayer resist edge. The silicon nitride was milled by FIB in areas where the bottom Au lines are visible in this image to form the nanowell. The circles are alignment marks.

whereas vapor-phase deposition methods were compatible with the prepatterned resist layers and did not disrupt the electrical characteristics of the active device regions. Furthermore, metal deposition and patterning on the vapor-phase-deposited SAMs was accomplished with a relatively large number of working devices free of electrical shorts or opens (yield is 15–20% per run for individual devices). Finally, this method was compatible with the use of multiple underlying layers of circuitry for insulated bottom contacts and patterned top contacts, as long as vapor deposition of SAMs and metal layers followed by lift off were the final steps. Hence, the process lends itself rather easily to the fabrication of complex, high-density circuits. Ellipsometry, scanning tunneling microscopy (STM), and X-ray photoelectron spectroscopy (XPS) were used to confirm the consistent deposition of a single, dense, chemisorbed, ordered, and uncontaminated monolayer of OPEs, as reported previously [26].

C. Room-Temperature Electrical Characterization of Interconnected Devices

The electrical behavior of plain-OPE molecular devices was studied by testing each cross-wire molecular device junction, first as individual devices, and then as interconnected devices in series and parallel, and then once again as individual devices to confirm that the I - V characteristics were preserved. Fig. 5

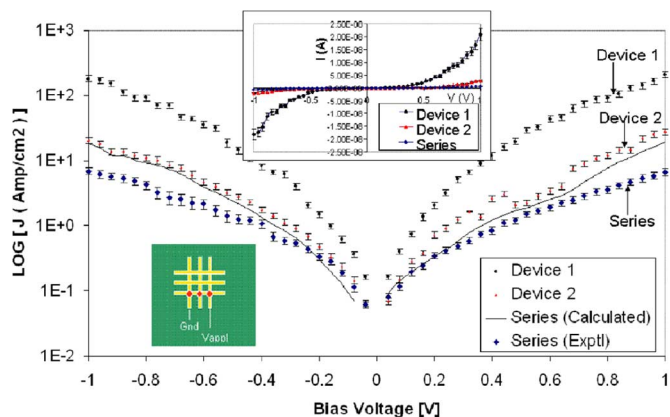


Fig. 5. Current density–voltage ($\log(J)$ versus V) characteristics (inset shows current–voltage, I – V) characteristics for a series crossbar circuit with molecular devices made from plain-OPE monolayers. Upon interconnection of device 1 (high conductance as judged by high current values of up to ~ 20 nA at 1 V, as shown by black circle symbols) to device 2 (low conductance device as judged by low current values of up to ~ 3 nA at 1 V, as shown by lighter triangular symbols), the characteristics of the series circuit shows lower current values than either of the devices (up to ~ 0.7 nA at 1 V). The calculated characteristics for the devices in series as sum of resistance of each individual device are also shown. Error bars are based on standard deviations from multiple measurements on the same device, before and after interconnection for the case of individual devices.

shows example I – V characteristics from individual devices. For purpose of comparison with nitro-OPE characteristics, we picked two types of devices: one with a “high current” level (device 1) and another with a “low current” level (device 2). These differences in current values between the various individual molecular devices can be attributed primarily to the different sizes of the nanowell device structures, as verified by scanning electron microscopy (SEM). Since “current density” numbers in Fig. 5 were calculated assuming a constant nanowell size (100 nm), whereas, in reality, these vary based on ion beam milling conditions as well as on the quality and thickness of the silicon nitride layer that are difficult to control, these are shown in Fig. 5, as devices with differing current density, whereas these occur due to differences in current from each device. Other less important conditions contributing to the variation molecular device junction current values include the chemical environment around molecules [27], and surface coverage variations of the monolayers. Next, we aimed to test for interconnection of devices by determining whether equivalent resistance of the two devices in series or parallel followed the trends expected for classical resistors. The characteristics based on calculated series resistance obtained from the addition of resistances from each individual device compares well in Fig. 5 with the experimentally determined device characteristics for the interconnected device in series, where current values were far less than that of either individual device. Subsequent retesting of the same individual devices showed that their electrical resistances remained the same, thus indicating that the molecular devices retained their individual electrical characteristics throughout testing.

Along similar lines, Fig. 6 shows that the current from interconnected devices in parallel was slightly higher than the current from the individual devices; and the experimentally de-

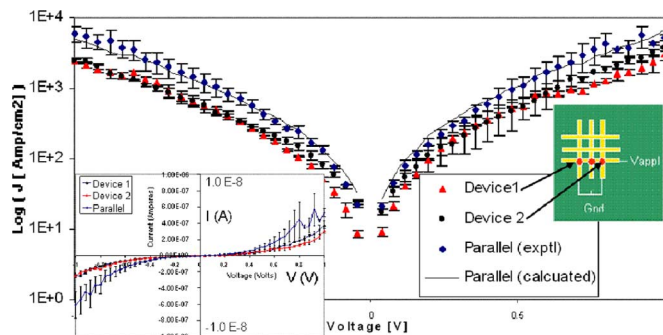


Fig. 6. Current density–voltage ($\log(J)$ versus V) characteristics (inset shows current–voltage, I – V) data from a parallel crossbar circuit with molecular devices made from single monolayer of OPEs, showing characteristics from two individual devices (with current values up to ~ 250 nA and ~ 320 nA at 1 V) and the interconnected device in parallel showing a higher current value (up to ~ 500 nA at 1 V). The calculated characteristics for the devices in parallel as sum of individual device current values are also shown. Error bars are based on standard deviations from multiple measurements on the same device, before and after interconnection for the case of individual devices.

termined characteristics agree well with the calculated characteristics based on equivalent resistance for devices interconnected in parallel. For the purpose of testing of interconnected series or parallel devices, although it was possible to fabricate in parallel all of the nine devices within each crossbar cell, within this work, nanowells were fabricated serially only for three devices within a row as shown in the green shaded insets of Figs. 5 and 6. This serial nanowell fabrication scheme was necessary during the initial testing phase to screen for “shorts,” thereby ensuring that the devices were electrically isolated from one another in the crossbar interconnection scheme and in this manner avoiding any alternate current pathways other than the interconnection line. Upon improvement of process yields (lesser number of “shorts”), we envision that the nanowell fabrication and lift off can be accomplished in a parallel manner.

D. Temperature-Dependent I – V Characterization of Individual Molecular Devices

Temperature-dependent I – V characteristics were used primarily to study whether the observed characteristics resulted from molecular transport signatures or due to transport through filament formation at the metal contact. For this purpose, we studied molecular devices with two distinctly different room-temperature current–voltage characteristics, to confirm if the characteristics persist down to low temperatures, where Joule heating of the metallic area that spurs filament formation is absent. We first studied the electron transport mechanism of a monolayer of plain-OPE molecules in our nanowell device at temperatures between 50 and 275 K. As is apparent from the two sweeps at each temperature in Fig. 7, there was no switching between various conductivity values for a given device. The current was observed to decrease with temperature, as would be expected for thermally activated hopping transport for the 300–100 K range (below this temperature the dependence of conductivity on temperature is minimal, but we do not have sufficient data points). Similar behavior has been reported in prior work [28], [29].

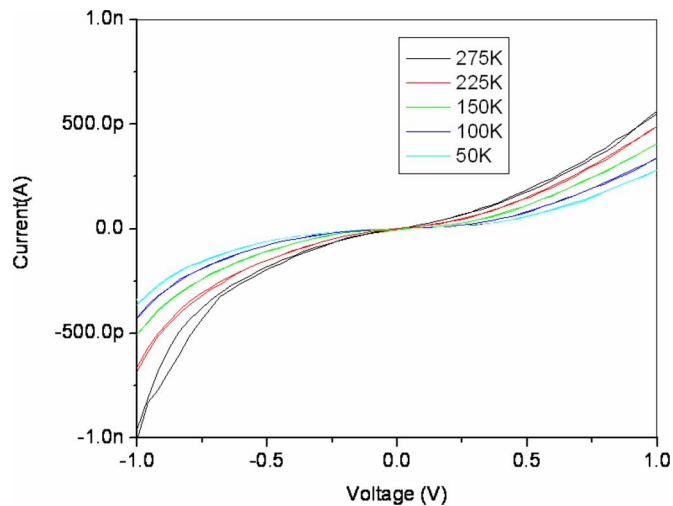


Fig. 7. Current–voltage characteristics of plain-OPE molecules within the nanowell device structure at different temperatures between 50 and 275 K. Multiple sweeps are shown to confirm that no switching was observed.

Next, we tested the nanowell device structure with the nitro-OPE SAM layer at temperatures between 100 and 300 K. As is apparent from Fig. 8(a), we observed switching with memory behavior for the entire temperature range, and this is similar to the room-temperature behavior as described elsewhere [24]. The current starts out in a “high” conductivity state, as shown by the label, “1st scan, 200 K,” and switches to a “low” conductivity state upon application of a threshold voltage of -1.75 V. The current remains in the “low” conductivity state during subsequent sweeps within the same voltage range as shown by the label “2nd scan, 200 K.” In order to reset the conductivity back to the “high” state a bias voltage greater than 1.5 V on the positive side was required, as is apparent from the scans labeled “3rd,” in inset of Fig. 8(a). Following the reset, current started again in the “high” state [“4th” scan of inset of Fig. 8(a)] and could be switched to the “low” state upon application of negative threshold voltage, as seen for “1st” and “2nd” scans at 150 K.

The negative-voltage scan region is enlarged in Fig. 8(b) to demonstrate that the switching characteristics persist down to low temperatures (100 K). However, the threshold voltage for switching increases as the temperature decreases, indicating that more external energy needs to be supplied to switch the molecular device, as the internal energy decreases with decreasing temperatures.

Recently, it has been suggested that filament formation at the metal–molecule interface may be responsible for the switching behavior of some molecular devices [17]. Since filament formation occurs due to Joule heating of a large metallic area [21], it should not be observed at low temperatures. Our observations of switching with memory behavior for nitro-OPE devices, down to low temperatures (100 K), suggest that the switching behavior is unlikely to be caused by the filament formation. Furthermore, since the same device structure and fabrication process were used for nanowell nitro-OPE and plain-OPE devices, and switching was observed down to 100 K, only with the former

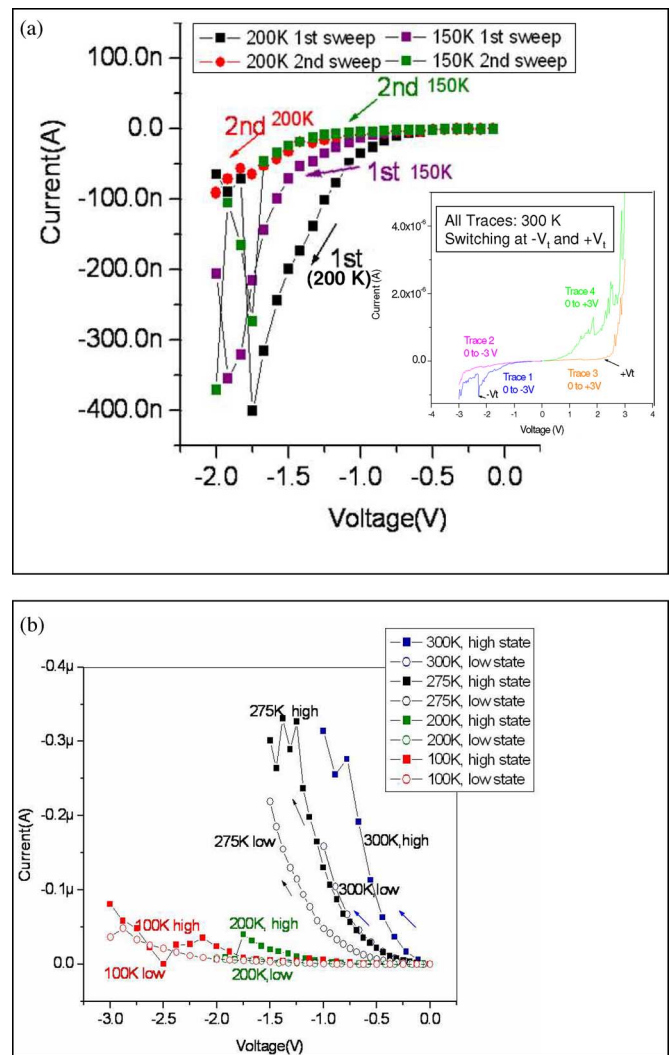


Fig. 8. (a) Switching behavior observed from nitro-OPE molecular devices at 200 and 150 K. Inset shows switching at $(-V_t)$ and $(+V_t)$ for molecular devices. (b) Switching persists down to 100 K, but the threshold voltage for switching is shifted to higher voltages for molecular junctions at lower temperatures.

and not with the latter, we hence conclude that the switching and other device characteristics that we observed herein were a characteristic signature of the molecular layer within the device structure and not of phenomena at the contacts, such as filament formation (since the latter would be the same for both nitro-OPE and plain-OPE devices).

IV. CONCLUSION

A process sequence based on a combination of vapor-phase deposition of molecular device layers and liftoff patterning techniques used in microelectronics was developed to enable massively parallel fabrication of a large number of interconnected planar nanowell molecular devices. The process was engineered for chemical compatibility of the resists with vapor-phase molecular deposition of a plain-OPE molecular layer and for permitting top-contact patterning through resist liftoff using a bilayer-resist process. Interconnection of molecular devices in series and parallel configurations was confirmed by I – V

characteristics similar to classical resistors with equivalent conductivity of each individual molecular device. To verify if the observed device characteristics were molecular transport signatures rather than transport through filament formation at the metal contact, individual molecular devices with two distinctly different room-temperature I - V characteristics, and nonswitching plain-OPE and switching nitro-OPE molecular devices, were studied as a function of temperature. Based on the persistence of the device characteristics of the respective molecule down to 100 K, we conclude that the transport mechanism observed within our device structure was a characteristic molecular signature of the respective molecule in the device structure and not filaments at the contacts, since Joule heating of the metallic area that spurs filament formation was less likely at low temperatures.

ACKNOWLEDGMENT

Assistance and advice from the research group of Prof. L. Pu of University of Virginia for storage and processing of chemicals and from UC Santa Barbara Microfabrication Laboratory for deposition of silicon nitride layers are acknowledged.

REFERENCES

- [1] ITRS Roadmap [Online]. Available: http://www.itrs.net/Links/2006Update/FinalToPost/00_ExecSum2006Update.pdf
- [2] V. V. Zhirnov, J. A. Hutchby, G. I. Bourianoff, and J. E. Brewer, "Emerging research logic devices," *IEEE Circuits Devices Mag.*, vol. 21, no. 3, pp. 37–46, May/Jun. 2005.
- [3] M. Forshaw, R. Stadler, D. Crawley, and K. Nikolic, "A short review of nanoelectronic architectures," *Nanotechnology*, vol. 15, no. 4, pp. S220–S223, 2004.
- [4] M. R. Stan, P. D. Franzon, S. C. Goldstein, J. C. Lach, and M. M. Ziegler, "Molecular electronics: From devices and interconnect to circuits and architecture," *Proc. IEEE*, vol. 91, no. 11, pp. 1940–1957, Nov. 2003.
- [5] J. R. Heath, P. J. Kuekes, G. S. Snider, and R. S. Williams, "A defect-tolerant computer architecture: Opportunities for nanotechnology," *Science*, vol. 280, no. 5370, pp. 1716–1721, 1998.
- [6] T. Hogg and G. S. Snider, "Defect-tolerant adder circuits with nanoscale crossbars," *IEEE Trans. Nanotechnol.*, vol. 5, no. 2, pp. 97–100, Mar. 2006.
- [7] D. F. Bocian, W. G. Kuhr, and J. Lindsey, "High-density non-volatile memory device," U.S. Patent 6657 884, 2003.
- [8] D. F. Bocian, W. G. Kuhr, and J. Lindsey, "High-density non-volatile memory device," U.S. Patent 6381 169, 2002.
- [9] K. W. Hipps, "Molecular electronics—It's all about contacts," *Science*, vol. 294, no. 5542, pp. 536–537, 2001.
- [10] B. Boer, M. M. Frank, Y. J. Chabal, W. Jiang, E. Garfunkel, and Z. Bao, "Metallic contact formation for molecular electronics: Interactions between vapor-deposited metals and self-assembled monolayers of conjugated mono- and dithiols," *Langmuir*, vol. 20, pp. 1539–1542, 2004.
- [11] B. C. Haynie, A. V. Walker, T. B. Tighe, D. L. Allara, and N. Winograd, "Adventures in molecular electronics: How to attach wires to molecules," *Appl. Surf. Sci.*, vol. 203, pp. 433–436, 2003.
- [12] S.-C. Chang, Z. Li, C. N. Lau, B. Larade, and R. S. Williams, "Investigation of a model molecular-electronic rectifier with an evaporated Ti-metal top contact," *Appl. Phys. Lett.*, vol. 83, pp. 3198–3200, 2003.
- [13] G. Y. Jung, S. Ganapathiappan, X. Li, D. A. A. Ohlberg, D. L. Olynick, Y. Chen, W. M. Tong, and R. S. Williams, "Fabrication of molecular-electronic circuits by nanoimprint lithography at low temperatures and pressures," *Appl. Phys. A Mater. Sci. Process.*, vol. 78, no. 8, pp. 1169–1173, 2004.
- [14] Y. Chen, G. Y. Jung, D. A. A. Ohlberg, X. M. Li, D. R. Stewart, J. O. Jeppesen, K. A. Nielsen, J. F. Stoddart, and R. S. Williams, "Nanoscale molecular-switch crossbar circuits," *Nanotechnology*, vol. 14, no. 4, pp. 462–468, 2003.
- [15] W. Wu, G. Y. Jung, D. L. Olynick, J. Straznicky, Z. Li, X. Li, D. A. A. Ohlberg, Y. Chen, S. Y. Wang, J. A. Liddle, W. M. Tong, and R. S. Williams, "One-kilobit cross-bar molecular memory circuits at 30-nm half-pitch fabricated by nanoimprint lithography," *Appl. Phys. A Mater. Sci. Process.*, vol. 80, no. 6, pp. 1173–1178, 2005.
- [16] Z. H. Zhong, D. L. Wang, Y. Cui, M. W. Bockrath, and C. M. Lieber, "Nanowire crossbar arrays as address decoders for integrated nanosystems," *Science*, vol. 302, no. 5649, pp. 1377–1379, 2003.
- [17] R. F. Service, "Next-generation technology hits an early mid-life crisis," *Science*, vol. 302, pp. 556–559, 2003.
- [18] N. Majumdar, N. Gergel, D. Routenberg, J. C. Bean, L. R. Harriott, B. Li, L. Pu, Y. Yao, and J. M. Tour, "Nanowell device for the electrical characterization of metal-molecule-metal junctions," *J. Vac. Sci. Technol. B*, vol. 23, no. 4, pp. 1417–1421, 2005.
- [19] A. R. Elsharkawi and K. C. Kao, "Switching and memory phenomena in anthracene thin films," *J. Phys. Chem. Solids*, vol. 38, pp. 95–96, 1977.
- [20] G. Snider, "Computing with hysteretic resistor crossbars," *Appl. Phys. A Mater. Sci. Process.*, vol. 80, no. 6, pp. 1165–1172, 2005.
- [21] A. R. Elsharkawi and K. C. Kao, "Switching and memory phenomena in anthracene thin films," *J. Phys. Chem. Solids*, vol. 38, pp. 95–96, 1977.
- [22] M. A. Reed, J. Chen, A. M. Rawlett, D. W. Price, and J. M. Tour, "Molecular random access memory cell," *Appl. Phys. Lett.*, vol. 78, pp. 3735–3737, 2001.
- [23] C. Li, D. Zhang, X. Liu, S. Han, T. Tang, C. Zhou, W. Fan, J. Koehne, J. Han, M. Meyyappan, A. M. Rawlett, D. W. Price, and J. M. Tour, "Fabrication approach for molecular memory arrays," *Appl. Phys. Lett.*, vol. 82, pp. 645–647, 2003.
- [24] N. Gergel-Hackett, N. Majumdar, Z. Martin, N. Swami, L. R. Harriott, J. C. Bean, G. Pattanaik, G. Zangari, Y. Zhu, L. Pu, Y. Yao, and J. M. Tour, "Room temperature molecular memory observed from a nanowell device," *J. Vac. Sci. Technol. A*, vol. 23, pp. 880–885, 2005.
- [25] F. Camacho-Alanis, L. Wu, G. Zangari, and N. Swami, "Molecular junctions of ~ 1 nm device length on SAM-modified n- and p-GaAs," *J. Mater. Chem.*, vol. 18, pp. 5459–5467, 2008.
- [26] N. Gergel-Hackett, M. J. Cabral, T. L. Pernell, L. R. Harriott, J. C. Bean, B. Chen, M. Lu, and J. M. Tour, "Vapor phase deposition of oligo (phenylene ethynylene) molecules for use in molecular electronic devices," *J. Vac. Sci. Technol. B*, vol. 25, no. 1, pp. 252–257, 2007.
- [27] N. Gergel-Hackett, N. Majumdar, Z. Martin, N. Swami, L. R. Harriott, J. C. Bean, G. Pattanaik, G. Zangari, Y. Zhu, L. Pu, Y. Yao, and J. M. Tour, "The effects of molecular environments on the electrical switching with memory of nitro-containing OPEs," *J. Vac. Sci. Technol. A*, vol. 24, no. 4, pp. 1243–1248, 2006.
- [28] J. Chen, L. C. Calvet, M. A. Reed, D. W. Carr, D. S. Grubisha, and D. W. Bennett, "Electronic transport through metal-1,4-phenylene diisocyanide-metal junctions," *Chem. Phys. Lett.*, vol. 313, pp. 741–748, 1999.
- [29] Y. Selzer, M. A. Cabassi, T. S. Mayer, and D. L. Allara, "Thermally activated conduction in molecular junctions," *J. Am. Chem. Soc.*, vol. 126, pp. 4052–4053, 2004.



Zena L. Martin received the B.S. and a M.S. in electrical engineering from the University of Virginia (UVA), Charlottesville, in 2004 and 2006, respectively.

Her current research interests include fabrication of device structures for molecular electronic. Most recently, she was a Photolithography Process Engineer with Qimonda.



Nabanita Majumdar received the B.S. degree in chemical engineering from Jadavpur University, Kolkata, India, and the M.S. degree in materials science and the Ph.D. degree in electrical engineering from the University of Virginia (UVA), Charlottesville.

She was engaged in fabrication and characterization of molecular electronic devices. She was a Process Integration Engineer, Micron Technology, Manassas, VA, and a Product Engineer at Qimonda, Richmond, VA.



Michael J. Cabral received the B.A. degree in physics from the Central College, Pella, IA, in 1995, the B.S. degree in electrical engineering from Washington University in St. Louis, St. Louis, MO, in 1996, the M.S. and Ph.D. degrees in electrical engineering from the University of Virginia (UVA), Charlottesville, in 2003 and 2004, respectively.

He is currently a Research Scientist in the Charles L. Brown Department of Electrical and Computer Engineering, University of Virginia (UVA). His current research interests include novel nanofabrication techniques using electron beam lithography and their application to the fabrication of molecular electronic devices.

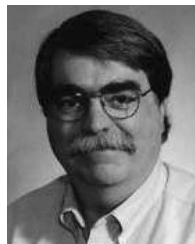


John C. Bean (M'81–SM'89–F'91) is currently the John Marshall Money Professor of electrical engineering with the University of Virginia (UVA), Charlottesville. As a member of the scientific staff of the Physics Research Division, Bell Laboratories, he pioneered techniques for the growth of silicon–germanium heterostructures and continues to explore the physical properties of these materials and their application in devices ranging from heterojunction bipolar transistors to resonant cavity photodiodes.



Nadine Gergel-Hackett received the B.S. and Ph.D. degrees from the Charles L. Brown Department of Electrical and Computer Engineering, University of Virginia (UVA), Charlottesville, in 2002 and 2006, respectively.

She was a Research Associate through a National Research Council Associate Award at the National Institute of Standards and Technology, Gaithersburg, MD, where she is currently an electrical engineer. Her current research interests include hybrid nontraditional and traditional materials, devices, and electronics, and novel memory devices.



Lloyd R. Harriott is the Virginia Microelectronics Consortium Professor at the University of Virginia (UVA), Charlottesville, and the Chair of the Department of Electrical and Computer Engineering, University of Virginia (UVA). He was a member of the scientific staff of Bell Laboratories, where he was a part of the team that was engaged in developing the EBES4 field emission electron beam lithography system for mask and wafer lithography. His current research interests include advancing nanolithography for the fabrication of nanoelectronic device platforms.

Y. Yao graduated from the University of South Carolina, Columbia (1994–1998).

He is currently a Synthetic Organic Chemist with Sigma-Aldrich, Madison, WI.



Fernanda Camacho-Alanis received the B.S. degree in chemical engineering in 2001 from the National University of Mexico, Mexico City, Mexico, from where she received the Master's degree in materials science in 2006. She is currently working toward the Ph.D. degree at the Department of Electrical Engineering, University of Virginia (UVA), Charlottesville.

She is currently completing her thesis on the fabrication of molecular electronic devices on semiconductor substrates, for the modulation of semiconductor band bending.

Ms. F. Camacho-Alanis won an Award for Excellence in Scholarship at UVA in 2009.



James M. Tour received the B.Sc. degree in chemistry from Syracuse University, Syracuse, NY, the Ph.D. degree in synthetic organic and organometallic chemistry from Purdue University, West Lafayette, IN.

He is currently the Chao Professor of chemistry at Rice University, Houston, TX. His current research interests include molecular electronics, nanotubes for health applications, chemical self-assembly, hydrogen storage on carbon nanotubes, synthesis of molecular motors and nanocars. He was a Postdoctoral

Trainee in synthetic organic chemistry at the University of Wisconsin, Madison, and Stanford University, Stanford, CA.



Nathan Swami received the Ph.D. degree from the University of Southern California, Los Angeles.

He was a Senior Scientist at the Clinical Microsensors, Inc., and a Principal Scientist at the Motorola Laboratories where he was engaged in interfacing biomolecules to microelectronic platforms. He is currently an Assistant Professor of electrical engineering with the University of Virginia (UVA), Charlottesville, where his research program focuses on the fabrication of electrical interfaces to molecular and biomolecular nanostructures for purposes of signal

transduction, guided self-assembly, and biomaterials synthesis. He was engaged in the fabrication of device structures based on carbon nanomaterials.

D. Long, photograph and biography not available at the time of publication.

R. Shashidhar, photograph and biography not available at the time of publication.